ISSN 1970-8734
Special Issue on *Heat Transfer*, Vol. 7 N. 2
February 2013

International Review of Mechanical Engineering (IREME)

REPRINT

Contents:

Guest Editorial Board 269

Aim and Topics of the Special Issue 270

Editorial 271
by Alina Adriana Minea (Guest Editor)

Numerical Analysis on Heat Transfer Enhancement and Wall Shear Stress of an Alumina Nanofluid for Different Forced Convection Flows 272
by Alina A. Minea, Oronzio Manca

Model-Based Approach for Investigation of Ladle Lining Damages 276
by Emil G. Mihailov, Venko I. Petkov, Ivan V. Doichev, Kosta P. Boshnakov

Determination of Stationary Temperature Distribution in Shielded Cables of Finite Length 282
by Florian Loos, Karl Dvorsky, Hans-Dieter Ließ

Analysis and Modeling of Heat Generation in Overcharged Li-Ion Battery with Passive Cooling 293
by Paul T. Coman, Christian T. Veje

Liquid Internal Cooling of High-Power Synchronous Permanent Magnet Generator Winding in Arctic Conditions 301
by M. Polikarpova, P. Röyttä, J. Pyrhönen

Enhancement of Heat Transfer through Jet Impingement by Using Detached Ribs 308
by Anupam Dewan, Deep Prakash Gupt, Sanjeev Sanghi

Two Dimensional Effects and Design Criteria with Biot and Transfer Number for Circular (Annular) Fins Having Internal Heat Generation Density 318
by Eleutherios N. Georgiou, Kypros F. Milidonis

eXtended Discrete Element Method Used for Convective Heat Transfer Predictions 328
by Alvaro A. Estupinan Donoso, Florian Hoffman, Bernhard Peters

Numerical Study of Turbulent Heat Transfer in Separated Flow: Review 337
by Hussein Togun, Tuqa Abdulrazzaq, S. N. Kazi, Abdul Amir H. Kadhum, Ahmed Badarudin, M. K. A. Ariffin, Emad Sadeghinezhad

(continued on inside back cover)

Praise Worthy Prize

Copyright © 2013 Praise Worthy Prize S.r.l. - All rights reserved

International Review of Mechanical Engineering (IREME)

Managing Editor:

Santolo Meo
Department of Electrical Engineering
FEDERICO II University
21 Claudio - I80125 Naples, Italy
santolo@unina.it

Editorial Board:

Jeongmin Ahn	(U.S.A.)	**Marta Kurutz**	(Hungary)
Jan Awrejcewicz	(Poland)	**Herbert A. Mang**	(Austria)
Ali Cemal Benim	(Germany)	**Josua P. Meyer**	(South Africa)
Stjepan Bogdan	(Croatia)	**Bijan Mohammadi**	(France)
Andrè Bontemps	(France)	**Hans Müller-Steinhagen**	(Germany)
Felix Chernousko	(Russia)	**Eugenio Oñate**	(Spain)
Kim Choon Ng	(Singapore)	**Pradipta Kumar Panigrahi**	(India)
Horacio Espinosa	(U.S.A)	**Constantine Rakopoulos**	(Greece)
Izhak Etsion	(Israel)	**Raul Suarez**	(Spain)
Michael I. Friswell	(U.K.)	**David J. Timoney**	(Ireland)
Nesreen Ghaddar	(Lebanon)	**George Tsatsaronis**	(Germany)
Adriana Greco	(Italy)	**Alain Vautrin**	(France)
Carl T. Herakovich	(U.S.A.)	**Hiroshi Yabuno**	(Japan)
David Hui	(U.S.A.)	**Tim S. Zhao**	(Hong Kong)
Heuy-Dong Kim	(Korea)		

The ***International Review of Mechanical Engineering (IREME)*** is a publication of the **Praise Worthy Prize S.r.l..**
The Review is published bimonthly, appearing on the last day of January, March, May, July, September, November.

Published and Printed in Italy by **Praise Worthy Prize S.r.l.,** Naples, February 28, 2013.

Copyright © 2013 Praise Worthy Prize S.r.l. - All rights reserved.

This journal and the individual contributions contained in it are protected under copyright by **Praise Worthy Prize S.r.l.** and the following terms and conditions apply to their use:
Single photocopies of single articles may be made for personal use as allowed by national copyright laws.
Permission of the Publisher and payment of a fee is required for all other photocopying, including multiple or systematic copying, copying for advertising or promotional purposes, resale and all forms of document delivery. Permission may be sought directly from **Praise Worthy Prize S.r.l.** at the e-mail address:
administration@praiseworthyprize.com

Permission of the Publisher is required to store or use electronically any material contained in this journal, including any article or part of an article. Except as outlined above, no part of this publication may be reproduced, stored in a retrieval system or transmitted in any form or by any means, electronic, mechanical, photocopying, recording or otherwise, without prior written permission of the Publisher. E-mail address permission request:
administration@praiseworthyprize.com

Responsibility for the contents rests upon the authors and not upon the **Praise Worthy Prize S.r.l.**.
Statement and opinions expressed in the articles and communications are those of the individual contributors and not the statements and opinions of **Praise Worthy Prize S.r.l.**. **Praise Worthy Prize S.r.l.** assumes no responsibility or liability for any damage or injury to persons or property arising out of the use of any materials, instructions, methods or ideas contained herein.
Praise Worthy Prize S.r.l. expressly disclaims any implied warranties of merchantability or fitness for a particular purpose. If expert assistance is required, the service of a competent professional person should be sought.

PREPRINT

Praise Worthy Prize

International Review of Mechanical Engineering (I.RE.M.E.), Vol. 7, N. 2
ISSN 1970 - 8734 Special Issue on Heat Transfer, February 2013

Enhancement of Heat Transfer through Jet Impingement by Using Detached Ribs

Anupam Dewan, Deep Prakash Gupt, Sanjeev Sanghi

Abstract – *Impinging jets provide an effective and flexible way to transfer thermal energy in various industrial applications. A computational investigation on the enhancement of heat transfer in air jet impingement over a flat smooth surface using detached ribs is performed in the present paper. The function of ribs is to make the flow turbulent, which results in an enhancement of the heat transfer. Fluid flow and heat transfer characteristics are studied in the computational domain using the RANS equations. It is observed that the accelerating fluid in the clearance between the ribs and plate causes a significant increase in the local turbulence and flow recirculation and these lead to an increased local heat transfer. A comparison of turbulence intensity and velocity profile at different sections in the vicinity of the ribs is performed. It is observed that none of the four turbulence models considered, namely, the standard k-ε model, RNG k-ε model, realizable k-ε model and k-ω model, accurately capture the variation of the local Nusselt number along the plate. However, the standard k-ε model performs the best.* ***Copyright © 2013 Praise Worthy Prize S.r.l. - All rights reserved.***

Keywords*: Enhanced Heat Transfer, Turbulence, CFD, k-ε Turbulence Model, Impingement*

I. Introduction

Heat transfer enhancement is getting increasing importance since the last few years as this technique increases the performance of any system which uses thermal energy, such as, internal combustion engines, food processing equipments, etc. Jet impingement is widely used in various industrial applications to achieve their desired heat and mass transfer characteristics. It provides an effective means for the enhancement of convective processes due to the high heat and mass transfer rates that can be achieved.

It performs better compared to those methods which use the same amount of fluid flowing parallel to the target surface. During the past few years many investigations dealing with the impingement heat transfer have been reported in the literature.

Dewan *et al.* [1] have recently summarized the state-of-the art in the computation of turbulent jet impingement heat transfer. In the case of turbulent jet impingement heat transfer, fluid at high velocity impinges on the heated surface from which one wants to remove heat.

Due to high velocity, the flow is turbulent and consequently heat transfer increases. Such processes have become popular in some industrial applications, such as, drying of food products, textiles, films and papers and in printing processes, processing of some metals and glass, cooling of gas turbine blades and outer wall of the combustion chamber, cooling of electronic equipment, etc.

With impinging jets, some scientists have used modified surfaces to increase the heat transfer, e.g., they have used surface roughness, attached ribs and detached ribs. Based on several experimental studies reported in the literature, it can be concluded that in all such situations, these techniques enhance heat transfer. In the present paper, a computational study to consider the effect of detached rib on the heat transfer from a smooth surface has been reported. The function of rib is to make the flow turbulent, which results in an enhancement of the heat transfer. With the availability of powerful computational fluid dynamics (CFD) packages, it has become easy to investigate various impinging jets problems.

Extensive studies covering both experimental and computational aspects of turbulent impinging jets have been reported by several authors. Gardon and Akfirat [2] studied the effect of turbulence on the heat transfer between a two-dimensional jet and a flat plate. They also studied the heat transfer distribution due to the impingement of multiple two-dimensional jets and concluded that for circular jets and small nozzle to plate gap ($z/d < 4$) the Nusselt number may show relative minimum for the stagnation point. Hoogendoorn [3] proposed that for low nozzle to plate distance ($z/d < 5$), the maximum Nusselt number shifts from the stagnation point.

Sugawara *et al.* [4] studied the effect of free turbulence on heat transfer and they concluded that for turbulence intensity of 8%, the heat transfer coefficient levels off to a value about 55% higher than that obtained

Manuscript received and revised January 2013, accepted February 2013 *Copyright © 2013 Praise Worthy Prize S.r.l. - All rights reserved*

REPRINT

for a very small value of the free stream turbulence. Lytle and Webb [5] studied the local heat transfer distribution on the very low nozzle to plate distances (z/d < 0.1). They used very long piped nozzle to make sure that the flow is fully developed at the discharge. They concluded that for low nozzle-to-plate spacing (z/d < 0.25) and for high Reynolds number, the maximum Nusselt number tends to shift from the stagnation point to the point of secondary peaks.

Lee *et al.* [6] studied the effect of nozzle diameter and observed that the local Nusselt number increases in the region x/d < 0.5 with increasing diameter of nozzle. Katti and Prabhu [7] reported experimental investigations and analysis of local heat transfer distribution on a flat surface due to the jet impingement from a long piped nozzle. Hansen and Webb [8] studied the effect of modified surface on the average Nusselt number. They used different types of finned surface and concluded that the magnitude of the enhancement, as represented by the system effectiveness, is strongly dependent on the fin type. They obtained enhancements in the heat transfer relative to a smooth surface ranging from 1.5 to 4.5 times. Ekkad and Kontrovitz [9] studied the effect of the dimpled surface on the heat transfer between an array of circular jets and the flat plate.

They reported reduction in the heat transfer coefficient for the dimpled surface as compared to the smooth surface. Gau and Lee [10] reported the heat transfer augmentation in a slot jet impinging on square ribbed and triangular ribbed walls. They performed both flow visualization and local Nusselt number measurements and found a reduction in the heat transfer in the case of triangular rib due to formation of air bubble enclosing cavities near the stagnation point which was smaller than that in the case of flat plate. They stated that if impingement is used, flow becomes turbulent and it easily penetrates the cavities resulting in an increase in the heat transfer and reported that square ribs are superior to triangular ribs.

Huang and El-Genk [11] studied the effect of air impingement on flat plate surface and experimentally obtained the value of the local and average Nusselt numbers, particularly for small value of Reynolds number and jet spacing. They found that the value of Nusselt number varies with Reynolds number and geometric conditions of the impinging system. Some researchers have performed experimental studies on detached ribs. Liou *et al.* [12] and Liou *et al.* [13] studied different configurations of detached ribs on the walls in internal flows and reported improved thermal performance compared to that of the attached ribs. The flow visualization results of Liou *et al.* [13] showed the presence of recirculating flow immediately behind the detached rib. They also observed an asymmetric wake behind the rib because of an asymmetric flow area across the rib.

They showed that the vortex shedding promotes the mixing of fluid and hence leads to a higher level of heat transfer distributions.

Tsia and Hwang [14] studied the effect of thermal conductivity of the attached ribs in internal flow using thermally active material (aluminium ribs) and thermally non-active turbulators (wooden ribs). They concluded that higher enhancements with thermally active ribs are due to the rib conduction effects. Their experiments with fully detached ribs showed an enhancement in the heat transfer due to enhancement in turbulence. They reported shedding of vortices from the detached rib and the wall jets ejecting from the rib clearance. Katti and Prabhu [15] studied the effect of axisymmetric detached ribs by normal impingement of a circular jet. They studied the effects of various parameters, such as, the nozzle to plate distance (z/d), clearance of rib from the plate (c/d), height of the rib (e/d), width of the rib (w/d), rib distance from the axis of the nozzle, on the performance. They concluded that there is a continuous enhancement in the Nusselt number from the stagnation point up to the first detached rib for all the ribbed configurations studied.

Shi *et al.* [16] performed computational study of impingement heat transfer for a two-dimensional model.

They compared the results using the Reynolds-stress transport model (RSM) and the standard k-ε turbulence model and concluded that results obtained by using the two models had negligible difference and were in good agreement with the corresponding experimental results. Pathak *et al.* [17] studied different turbulence models for slightly heated jet discharged in a crossflow. They concluded that for three-dimensional flow, the computations using the Reynolds stress transport model performed better than those using the standard k-ε model. Sak *et al.* [18] investigated the effect of turbulence length scale and turbulence intensity on forced convection heat transfer from a heated horizontal circular cylinder.

In the present paper we have computationally investigated the effect of detached ribs on the heat transfer characteristics through a turbulent jet impingement over a smooth flat plate. The governing equations and turbulence models used are described in Section II. The computational domain, boundary conditions, grid independence study and code validation are reported in Section III. The effect of detached ribs, comparison of different turbulence models and flow features at different sections in the vicinity of the ribs are reported in Section IV followed by conclusions.

II. Mathematical Model

II.1. General Equations

Nu denotes the Nusselt number, which represents the non-dimensional form of the convective heat transfer coefficient h and is given as:

$$Nu = \frac{hd}{k} \tag{1}$$

Copyright © 2013 Praise Worthy Prize S.r.l. - All rights reserved

REPRINT

$$h = \frac{q_w}{T_w - T_0} \tag{2}$$

here q_w denotes the heat flux from the wall. T_0 and T_w denote the air jet temperature at inlet and temperature of wall, respectively, and d denotes the diameter of the discharge nozzle.

Numerical simulation of the flow and thermal fields in the present study requires the solutions of Reynolds-averaged governing equations for the conservation of mass, momentum and energy. In the Cartesian coordinate system these equations can be written for an incompressible fluid as:

Continuity Equation:

$$\frac{\partial U_i}{\partial x_i} = 0 \tag{3}$$

Momentum Equation:

$$\frac{\partial}{\partial x_j}\left(\rho \bar{U}_i \bar{U}_j\right) = -\frac{\partial P}{\partial x_i} + \frac{\partial}{\partial x_j}\left[\mu\left(\frac{\partial \bar{U}_i}{\partial x_j} + \frac{\partial \bar{U}_j}{\partial x_i}\right) - \rho\overline{u_i' u_j'}\right] \tag{4}$$

Energy Equation:

$$\frac{\partial}{\partial x_j}\left[\bar{U}_i\left(\rho E + p\right)\right] = \frac{\partial}{\partial x_j}\left[\left(k + \frac{c_p \mu_t}{Pr_t}\right)\frac{\partial T}{\partial x_j} + \bar{U}_i\left(\tau_{ij}\right)_{eff}\right] \tag{5}$$

where:

$$\left(\tau_{ij}\right)_{eff} = \mu_{eff}\left(\frac{\partial \bar{U}_j}{\partial x_i} + \frac{\partial \bar{U}_i}{\partial x_j}\right) - \frac{2}{3}\mu_{eff}\frac{\partial \bar{U}_k}{\partial x_k}\delta_{ij} \tag{6}$$

The unknown terms appearing on the right-hand sides of equations (4) and (5) are termed as the Reynolds stress tensor and turbulent heat fluxes, respectively.

These represent correlations between the (a) fluctuating velocities and (b) fluctuating velocities and fluctuating temperature, respectively. These are additional stress and turbulent transport terms due to turbulence (Dewan [19]). We need a model for these terms to close the system of the Eqs. (4) and (5).

Four popular turbulence models used for closing the system of equations are described here.

II.2. Standard k-ε Model

The standard *k-ε* model (Launder and Spalding [20]) is a two equation turbulence model in which two transport equations, one for the turbulence kinetic energy (k) and other for its dissipation rate (ε) are employed to calculate the eddy viscosity which is given by the expression $\mu_t = \rho c_\mu k^2/\varepsilon$ where C_μ denotes an empirical model constant:

$$\frac{\partial}{\partial x_i}\left(\rho k \overline{U_i}\right) = \frac{\partial}{\partial x_j}\left[\left(\mu + \frac{\mu_t}{\sigma_k}\right)\frac{\partial k}{\partial x_j}\right] + G_k - \rho\varepsilon \tag{7}$$

$$\frac{\partial}{\partial x_i}\left(\rho \varepsilon \overline{U_i}\right) = \frac{\partial}{\partial x_j}\left[\left(\mu + \frac{\mu_t}{\sigma_\varepsilon}\right)\frac{\partial \varepsilon}{\partial x_j}\right] + C_{1\varepsilon}\frac{\varepsilon}{k}\left(G_k\right) - C_{2\varepsilon}\rho\frac{\varepsilon^2}{k} \tag{8}$$

In Eqs. (7) and (8), G_k represents the generation of turbulence kinetic energy due to the mean velocity gradient. The values of the model constants used in these equations are:

$$C_\mu = 0.09, C_{1\varepsilon} = 1.44, C_{2\varepsilon} = 1.92, \sigma_k = 1.0, \sigma_\varepsilon = 1.31$$

(Launder and Spalding, [20]). Here σ_ε and σ_k denote the turbulent Prandtl numbers for ε and k, respectively. In the derivation of the *k-ε* model, the flow is assumed to be fully turbulent and the effects of molecular viscosity are negligible. The standard *k-ε* model is therefore valid only for fully turbulent and high Reynolds number flows.

II.3. Realizable k-ε Model

The realizable *k-ε* model (Shih *et al*., [21]) is modified form of the standard *k-ε* model and is different from the standard *k-ε* model in two ways:

(1) It uses a different formulation for the turbulent viscosity and

(2) A different transport equation for the dissipation rate ε is derived from an exact equation for the transport of the mean-square vorticity fluctuations:

$$\frac{\partial}{\partial x_i}\left(\rho k \overline{U_i}\right) = \frac{\partial}{\partial x_j}\left[\left(\mu + \frac{\mu_t}{\sigma_k}\right)\frac{\partial k}{\partial x_j}\right] + G_k - \rho\varepsilon - Y_M \tag{9}$$

$$\frac{\partial}{\partial x_i}\left(\rho \varepsilon \overline{U_i}\right) = \frac{\partial}{\partial x_j}\left[\left(\mu + \frac{\mu_t}{\sigma_\varepsilon}\right)\frac{\partial \varepsilon}{\partial x_j}\right] + \rho C_1 S_\varepsilon - \rho C_2 \frac{\varepsilon^2}{k + \sqrt{\nu\varepsilon}} \tag{10}$$

where $C_1 = max\ [0.43, \eta/(\eta+5)]$, $\eta = S\,k/\varepsilon$:

$$S_{ij} = \frac{\bar{U}_{i,j} + \bar{U}_{j,i}}{2},\ \tilde{S} = \sqrt{S_{ij}S_{ij}} \tag{11}$$

The model constant C_μ in the expression for the eddy viscosity:

REPRINT

Copyright © 2013 Praise Worthy Prize S.r.l. - All rights reserved

$$\mu_t = \rho C_\mu \frac{k^2}{\varepsilon} \tag{12}$$

depends on the rate of rotation tensor and strain tensor and is given as:

$$C_\mu = \frac{1}{A_0 + A_S \dfrac{kU^*}{\varepsilon}} \tag{13}$$

$$U^* = \sqrt{S_{ij}S_{ij} + \overline{\Omega}_{ij}\overline{\Omega}_{ij}} \tag{14}$$

where $\overline{\Omega}_{ij}$ denotes the rate of rotation tensor and A_0 and A_S denote the model constants. The values of the model constants are $C_{1\varepsilon} = 1.44$, $C_2 = 1.9$, $\sigma_k = 1.0$, $\sigma_\varepsilon = 1.2$ and $A_0 = 4.04$ (Shih *et al*. [21]).

II.4. RNG k-ε Model

The RNG *k-ε* model equations are similar to the standard *k-ε* model except there is the one additional term which relates the mean rate of strain and turbulence quantities (Yakhot *et al*. [22]). The RNG *k-ε* model mainly accounts for the effect of swirl on turbulence, uses an analytical formulation for the turbulent Prandtl number and a differential expression for the effective viscosity.

The following transport equations are employed. Turbulence kinetic energy:

$$\rho\bar{U}_i \frac{\partial k}{\partial x_i} = \mu_t S^2 + \frac{\partial}{\partial x_i}\left(\alpha_k \mu_{eff} \frac{\partial k}{\partial x_i}\right) - \rho\varepsilon \tag{15}$$

where:

$$S \equiv \sqrt{2S_{ij}S_{ij}}, \quad S_{ij} \equiv \frac{1}{2}\left(\frac{\partial \bar{U}_j}{\partial x_i} + \frac{\partial \bar{U}_i}{\partial x_j}\right) \tag{16}$$

Dissipation rate:

$$\rho\bar{U}_i \frac{\partial \varepsilon}{\partial x_i} = C_{1\varepsilon}\left(\frac{\varepsilon}{k}\right)\ \mu_t S^2 + \\ + \frac{\partial}{\partial x_i}\left(\alpha_\varepsilon \mu_{\text{eff}} \frac{\partial \varepsilon}{\partial x_i}\right) - C_{2\varepsilon}\rho\left(\frac{\varepsilon^2}{k}\right) - R \tag{17}$$

where the model constants are derived using the RNG theory.

II.5. Standard k-ω Model

In the standard *k-ω* model (Wilcox [23]) transport equation for turbulence kinetic energy *k* and the specific dissipation rate *ω* are solved. These transport equations may be written as:

$$\frac{\partial}{\partial x_i}\left(\rho k\bar{U}_i\right) = \frac{\partial}{\partial x_j}\left(\Gamma_k \frac{\partial k}{\partial x_j}\right) + G_k + Y_k \tag{18}$$

$$\frac{\partial}{\partial x_i}\left(\rho \omega\bar{U}_i\right) = \frac{\partial}{\partial x_j}\left(\Gamma_\omega \frac{\partial k}{\partial x_j}\right) + G_\omega + Y_\omega \tag{19}$$

In Eqs. (18) and (19), G_k represents the generation of turbulence kinetic energy due to the mean velocity gradient, G_ω represents the generation of specific dissipation rate. Γ_k and Γ_ω represent the effective diffusivity of k and ω, respectively.

III. Computational Domain and Boundary Conditions

Fig. 1(a) shows a schematic of the computational domain considered in the present study which is based on the experimental study of Katti and Prabhu [15]. The nozzle is considered to be of circular cross-section and ribs are assumed to be placed axisymmetrically. The flow and thermal fields are assumed to be symmetric about the axis.

The ribs are shown in Fig. 1(a) by hatched squares and the locations of different sections B, C, D and E chosen to determine the flow behavior near the ribs are also shown. Fig. 1(a) also shows the notations used in the present study. Fig. 1(b) shows the boundary conditions used in the present computations. At the nozzle the magnitude of velocity calculated from the corresponding value of the Reynolds number was specified. In the present computations a value of Reynolds number equal to 20000 was considered (Katti and Prabhu [15]). Target plate was considered as a solid wall made up of steel and the no slip condition was used.

It was maintained at a constant heat flux equal to 5000 W/m^2. The ribs were also specified as the solid walls with the corresponding no slip and adiabatic conditions.

At all the remaining boundaries of the computational domain the pressure equal to the atmospheric pressure was specified.

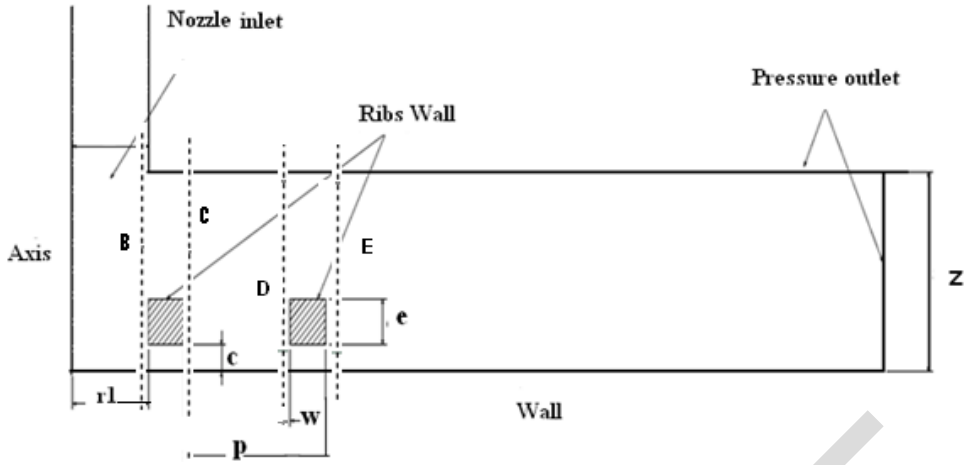
The computations were performed for the following values of the geometric parameters: Distance of the nozzle from the plate (z/d) = 0.5; width and height of rib (w/d = e/d) = 0.23; clearance from the flat surface (c/d) = 0.067; distance of the first rib from the axis of nozzle (r_1/d) = 0.5 and pitch of the rib p/e = 4.0 (Katti and Prabhu [15]).

III.1. Code Validation

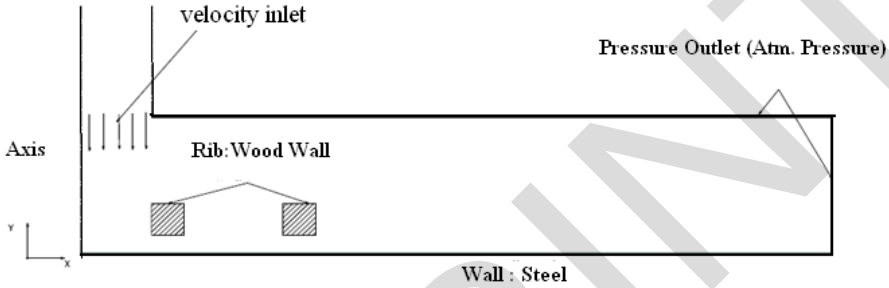
Shi *et al*. [16] performed a computational study of the jet impingement heat transfer under a turbulent slot jet (Fig. 2(a)) using the finite volume method (Patankar [24]). The present code was validated using the results of Shi *et al*. [16], who used symmetric, two-dimensional slot jet. The boundary conditions used for the code validation are shown in Fig. 2(b).

REPRINT

Copyright © 2013 Praise Worthy Prize S.r.l. - All rights reserved



(a)



(b)

Figs. 1. (a) Computational domain considered in the present study and (b) Boundary conditions considered in the present study

A slot of width (W) is used to impinge air on the target plate of length 2X which is kept at a distance of H from the slot. The values of the geometric parameters used in the computational study are: width of slot W = 7.5 mm, distance of the slot from the plate H/W = 12.0 and length of plate from axis of slot X/W = 50 (Shi *et al*. [16]).

In the present study, four different meshes with number of elements equal to 15668, 18996, 23596 and 32568 were considered in order to check the sufficiency of the mesh resolution for the above-mentioned case. We observe from Fig. 3 that for the two coarse meshes with number of elements equal to 15668 and 18996 the computed results show some variation in the heat transfer coefficient compared to those for other two fine meshes with number of elements equal to 23596 and 32568.

However, the results using two fine meshes are nearly coincident and therefore grid independent. Shi *et al*. [16] performed their computational investigation with a constant heat flux of 3490 W/m^2 and they discretized the governing equations using the first order upwind scheme and used the SIMPLEC algorithm for the pressure velocity coupling. They used the standard *k-ε* turbulence model with the standard wall functions as the near wall treatment.

In the present study the commercial software GAMBIT was used for the creation of geometry and meshing and finite volume based software FLUENT 6.3.26 was used for the solution of the governing equations. The same boundary conditions and turbulence models as those used by Shi *et al*. [16] were considered in the present study for the code validation.

Fig. 4 shows that the present grid independent computations of the heat transfer coefficient for Reynolds number equal to 12000 using 32568 elements are in good agreement with those of Shi *et al*. [16].

For the subsequent computations, we have used the second order upwind scheme and SIMPLE algorithm for the pressure-velocity coupling for the case of turbulent jet impinging on a plate mounted with detached ribs.

IV. Results and Discussion

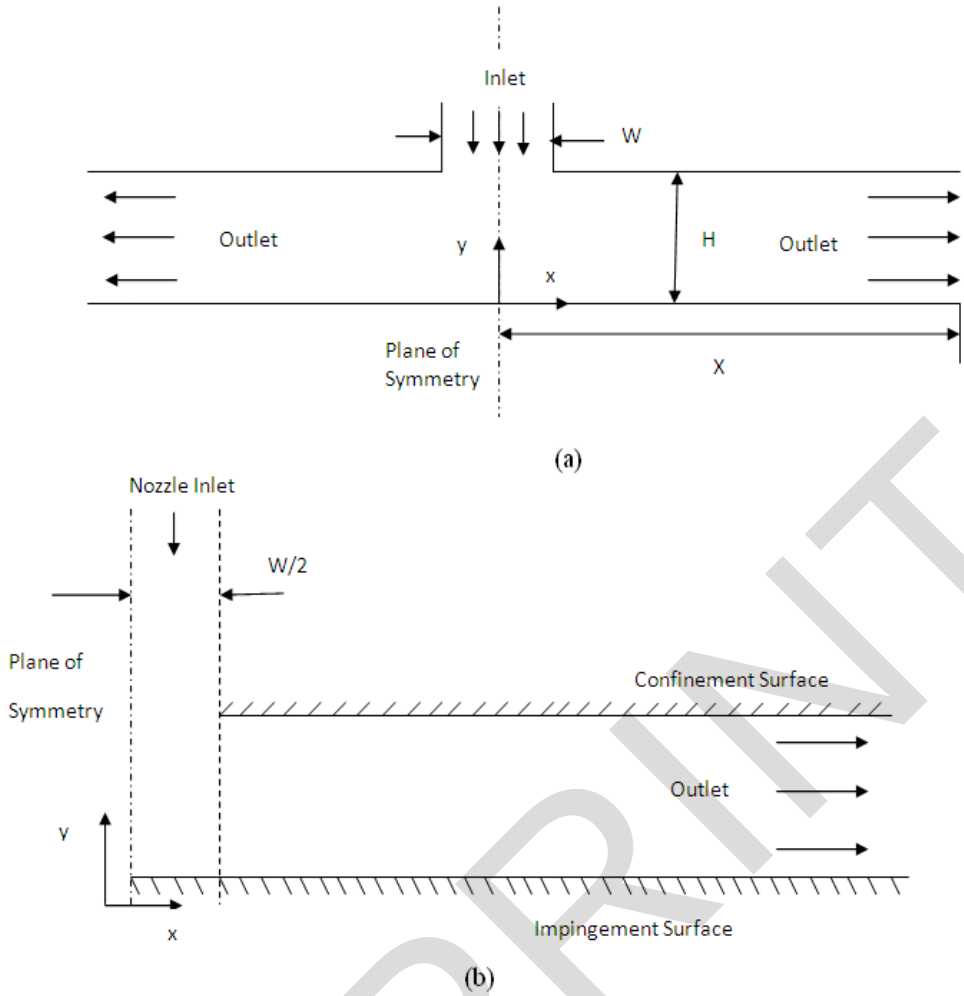
IV.1. Comparison of Different Turbulence Models

We first compared the performance of four widely used RANS equations based turbulence models, namely, the standard *k-ε* model, realizable *k-ε* model, RNG *k-ε* model (the enhanced wall functions were used for treating the near wall turbulence for these three turbulence models) and the standard *k-ω* model for the prediction of the local Nusselt number over the plate on which ribs were mounted.

As can be seen from Fig. 5, the standard *k-ε* model, realizable *k-ε* model and RNG *k-ε* model show nearly the same Nusselt number distribution while the standard *k-ω* model predicts a somewhat different behavior.

Copyright © 2013 Praise Worthy Prize S.r.l. - All rights reserved

REPRINT



Figs. 2. (a) Flow geometry of impingement considered by Shi *et al.* [16] and (b) Computational domain and boundary condition considered by Shi *et al*. [16]

The predicted maximum value of the Nusselt number occurs at x/d = 0.5 by all the models as compared to the maximum value of Nusselt number at x/d = 1.0 measured by Katti and Prabhu [15]. The reason behind such a performance by these turbulence models is that these do not accurately capture the complex turbulent flow field in the vicinity of the second detached rib (located at x/d = 1.4). However, the standard *k-ε* model and its two variants correctly predict the local Nusselt number near the first rid (located at x/d = 0.5). The standard *k-ω* model significantly overpredicts the Nusselt number in the vicinity of the stagnation region (x/d = 0). Therefore, the standard *k-ε* model with the enhanced near wall functions is used for all the subsequent computations.

IV.2. Effect of Detached Ribs

Next we present the effect of detached ribs on the heat transfer characteristics.

The computed values of Nusselt number in two cases, i.e., smooth heated plate without ribs and heated plate with detached ribs are shown in Fig. 6. It is observed that the detached rib significantly increases Nusselt number in the nozzle region (x/d = 0 to 1). As seen from Fig. 6, the peak value of Nusselt number is achieved just behind the first detached rib from the centre of the nozzle.

This is probably due to low clearance available and fluid flow through the clearance.

Thus a wake region is created just behind the first rib which is responsible for highly turbulent flow and results into high heat transfer and hence high Nusselt number (Fig. 6).

IV.3. Turbulence Intensity at Various Sections

The heat transfer from a heated plate depends on several factors, such as, the surface area, thermal conductivity of the plate as well as the heat transfer coefficient of the surrounding medium.

The heat transfer coefficient of the surrounding medium depends strongly on turbulence, which is characterized by turbulence intensity expressed as $I = u' / U$, where u' denotes the r.m.s. value of the velocity fluctuations in the flow and U the mean velocity.

In this section the effect of detached rib on turbulent intensity is examined.

Copyright © 2013 Praise Worthy Prize S.r.l. - All rights reserved

REPRINT

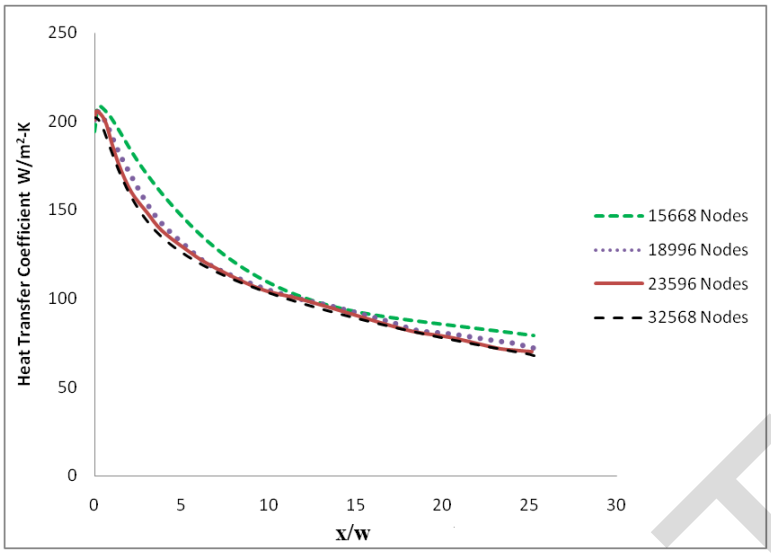


Fig. 3. Grid independence study

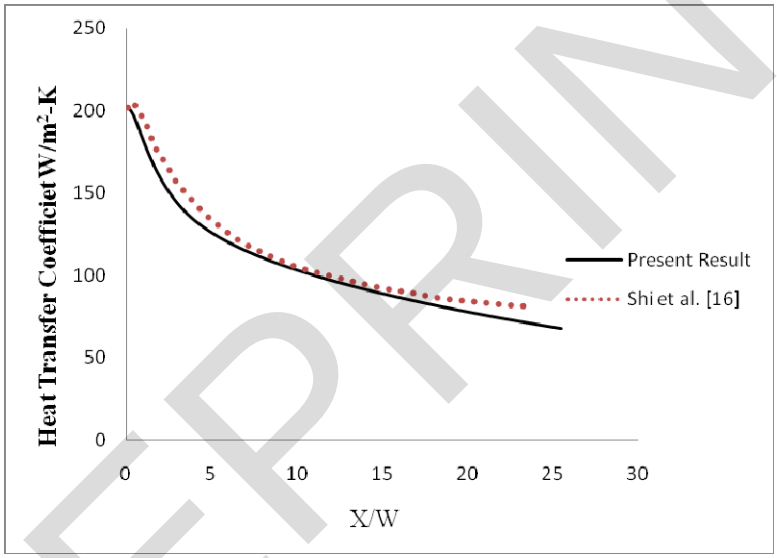


Fig. 4. Comparison of present computational results with those by Shi *et al.* [16]

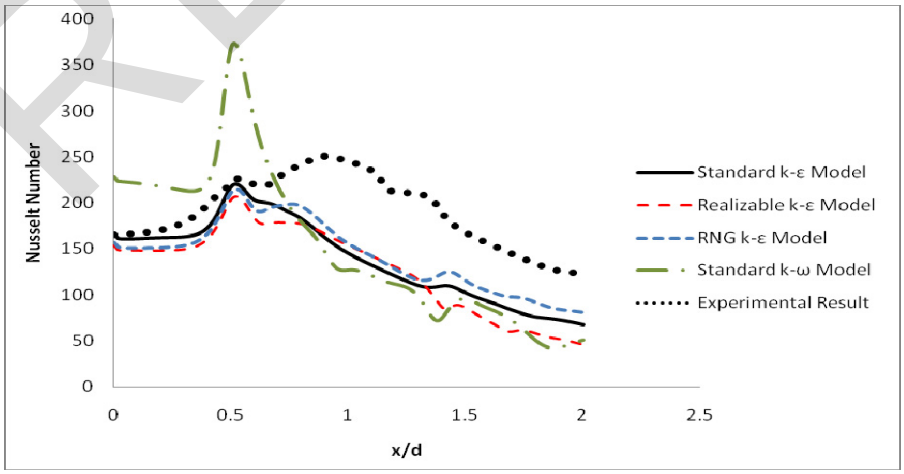


Fig. 5. Comparison of four turbulence models (experimental data of Katti and Prabhu [15] is used for comparison)

REPRINT

Copyright © 2013 Praise Worthy Prize S.r.l. - All rights reserved

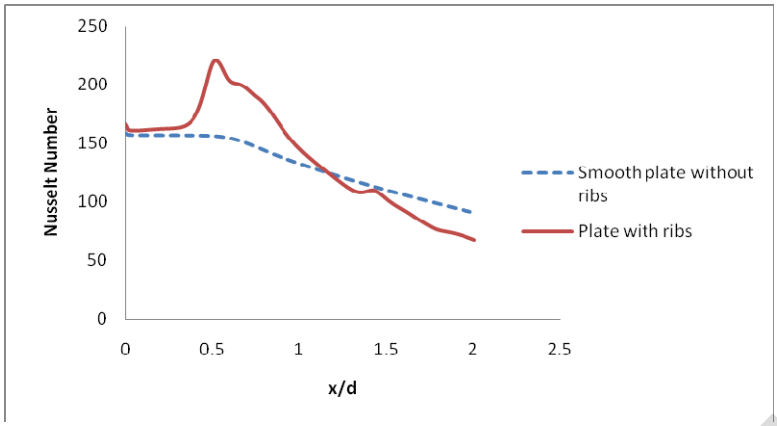


Fig. 6. Effect of detached rib on Nusselt number

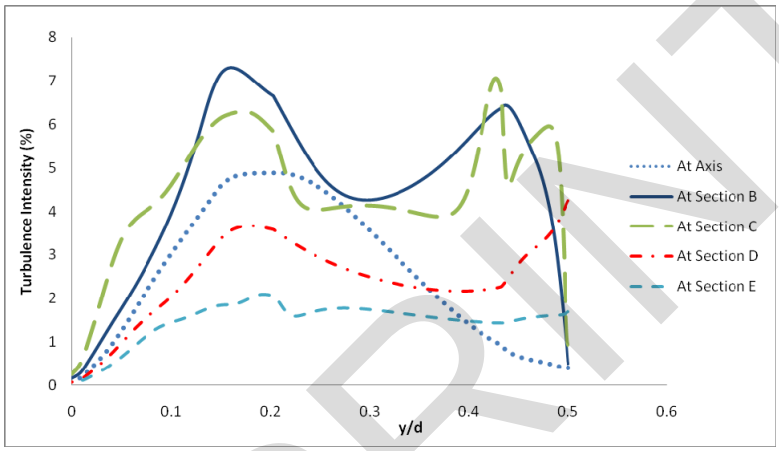


Fig. 7. Turbulence intensity variation at different sections

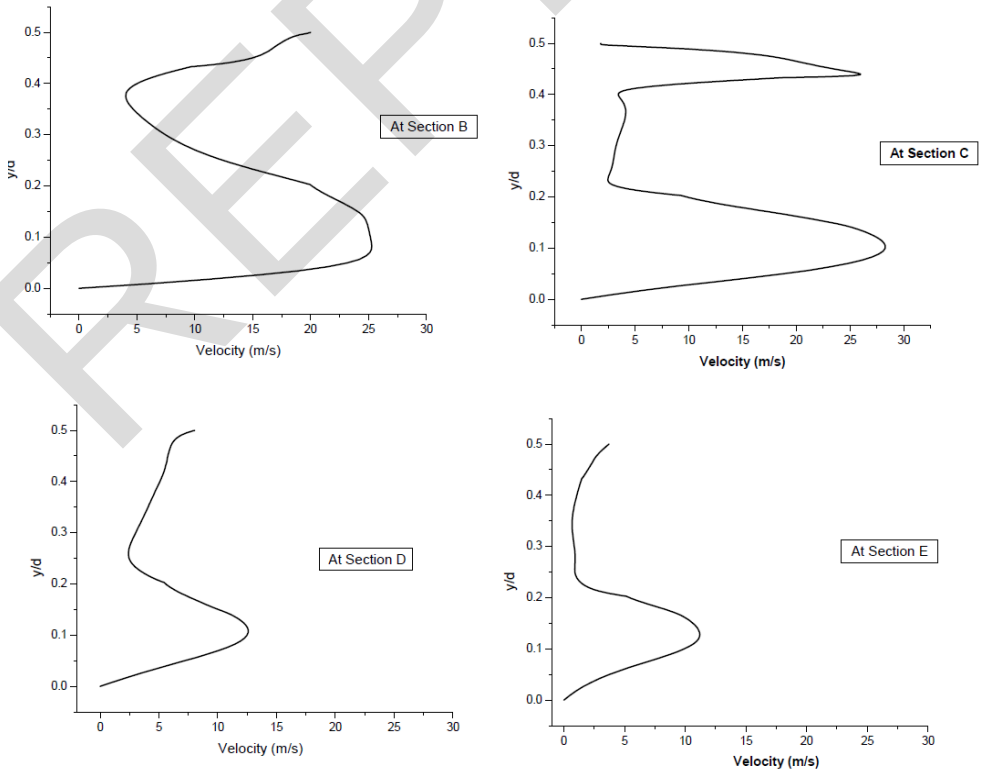


Fig. 8. Velocity distribution at different sections

REPRINT

Copyright © 2013 Praise Worthy Prize S.r.l. - All rights reserved

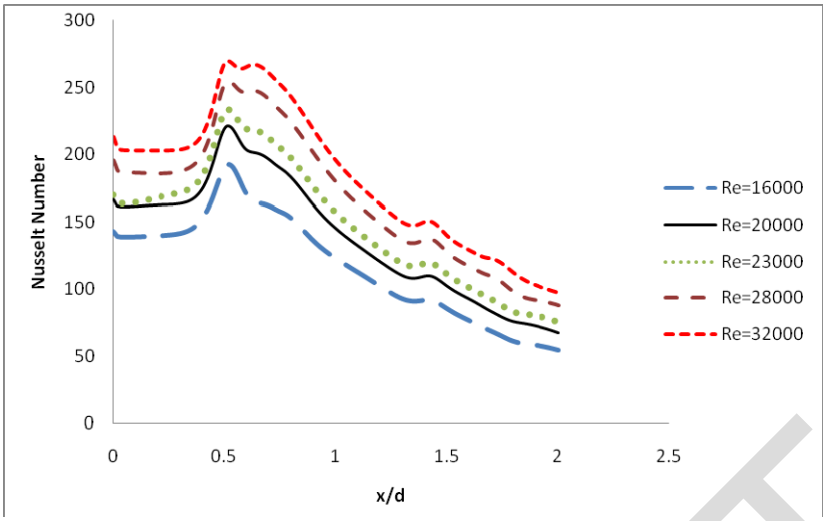


Fig. 9. Effect of jet Reynolds number on local Nusselt number distribution over the plate

Normal predicted variation of turbulence intensity is compared at five sections located at x/d = 0 (Axis), x/d = 0.46 (termed as section B), x/d = 0.77 (termed as section C), x/d = 1.38 (termed as section D) and x/d = 1.69 (termed as section E). As seen from Fig. 6 the heat transfer can be increased considerably by using a detached rib, which is due to corresponding increase in turbulence in air flow. Fig. 7 shows that the flow achieves the maximum turbulence intensity (~ 5%) at the axis immediately above the stagnation point and then its value decreases slowly to the value corresponding to the inlet conditions. Section B, which is located before the rib has a different scenario. Here the turbulence intensity increases to a maximum value (~ 7%) just above the plate. Nusselt number starts to increase just before the rib. Due to a small clearance between the plate and ribs, fluid gains velocity through the clearance. Hence just after the rib (at the section C), the intensity reaches its maximum level (~ 6%). Nusselt number is not at its peak value at this location, because most heat is removed by the fluid before the rib and the same air passes through the clearance. But due to such high turbulence intensity, small peak is shown in Nusselt number after the first rib (Section C). At the section D, turbulence intensity reaches the maximum value of 4%. At the section E, the turbulence intensity does not achieve a large value because the effect of swirl is not important in this region. Hence we can say that rate of heat transfer achieves considerable enhancement in between the sections B and D and the corresponding maximum value of Nusselt number for the plate is nearly equal to 220 (Fig. 6).

IV.4. Mean Velocity Distribution

We present here the physical behavior of fluid flow near the ribs and effect of velocity distribution on heat transfer rate at different sections near the ribs. At section B, the velocity becomes high due to flow acceleration occurring in the clearance between the plate and rib (Fig. 8). A sudden drop in velocity occurs (y/d = 0.4) and again the velocity increases up to the value equal to the inlet velocity. Similarly at sections C, D and E large velocity variations occur due to fluid gaining velocity in the vicinity of the plate and resulting good mixing due to flow recirculation and formation of wake behind ribs (Fig. 8). Thus the rate of convective heat transfer from the heated plate increases.

IV.5. Effect of Inlet Jet Reynolds Number on Nusselt Number

The heat transfer rate also depends on the discharge jet Reynolds number. Fig. 9 shows the local distribution of Nusselt number for five values of jets Reynolds number considered varying from 16000 to 32000.

It is observed that the value of Nusselt number increases with an increase in Reynolds number throughout the plate, which is due to fluid acceleration and flow recirculation near the ribs resulting in good mixing due to a high discharge velocity.

V. Conclusion

A computational study is performed to investigate the heat transfer between normally impinging turbulent circular air jet and a flat surface mounted with detached ribs. Four widely used RANS turbulence models, namely, the standard *k-ε* model, realizable *k-ε* model, RNG k-ε model and standard *k-ω* model, are considered. It is observed that none of the turbulence models considered could accurately capture the local variation of Nusselt number along the plate and this poor behavior could be due to the limitation of modeling complex turbulent flow using the Reynolds-Averaged Navier–Stokes (RANS) equations. Solution of unsteady, three-dimensional flow and thermal fields using large eddy simulation may provide better results for this flow configuration, but at a significantly large computational

PREPRINT

Copyright © 2013 Praise Worthy Prize S.r.l. - All rights reserved

cost. It is observed that there is a continuous enhancement in Nusselt number from the stagnation point up to the first detached rib. This is due to fluid gaining velocity in the stagnation region due to clearance under the first rib. Good mixing due to flow recirculation and vortex formation results in an increase in turbulence intensity. Further it has been observed that an increase in Reynolds number increases the heat transfer rate from the target plate.

References

[1] A. Dewan, R. Dutta and B. Srinivasan, Recent Trends in Computation of Turbulent Jet Impingement Heat Transfer, *Heat Transfer Engineering*, vol. 33, nos. 4 & 5, pp. 447–460, 2012.

[2] R. Gardon and C. Akfirat, The Role of Turbulence in Determining the Heat Transfer Characteristics of Impinging Jet, *Int. J. Heat Mass Transfer,* vol. 8, pp. 1261–1272, 1965.

[3] C.J. Hoogendoorn, The Effect of Turbulence on Heat Transfer at a Stagnation Point, *Int. J. Heat Mass Transfer*, vol. 20, pp. 1333-1338, 1977.

[4] S. Sugawara, T. Sato, H. Komatsu and H. Osaka, Effect of Free Stream Turbulence on the Flat Plate Heat Transfer, *Int. J. Heat Mass Transfer*, vol. 31, pp. 5-12, 1988.

[5] D. Lytle and B.W. Webb, Air Jet Impingement Heat Transfer at Low Nozzle Plate Spacing, *Int. J. Heat and Mass Transfer,* vol. 37, pp. 1687–1697, 1994.

[6] D.H. Lee, J. Song and J.C. Myeong, The Effect of Nozzle Diameter on Impinging Jet Heat Transfer and Fluid Flow, *Int. J. Heat mass Transfer,* vol. 126, pp. 554–557, 2004.

[7] V.V. Katti and S.V. Prabhu, Experimental Study and Theoretical Analysis of Local Heat Transfer Distribution between Smooth Flat Surface and Impinging Air Jet from a Circular Straight Pipe Nozzle, *Int. J. Heat Mass Transfer*, vol. 51, pp. 4480-4495, 2008.

[8] L.G. Hansen and B.W. Webb, Air Jet Impingement Heat Transfer from Modified Surfaces, *Int. J. Heat Mass Transfer,* vol. 36, pp. 989–997, 1993.

[9] S.V. Ekkad and D. Kontrovitz, Jet Impingement Heat Transfer on the Dimpled Target Surfaces, *Int. J. Heat and Fluid Flow*. vol. 23, pp. 22–28, 2002.

[10] C. Gau and C.C. Lee, Impingement Cooling Flow Structure and Heat Transfer along Rib-Roughened Walls, *Int. J. Heat and Mass Transfer,* vol. 35, no. 11, pp. 3009-3020, 1992.

[11] L. Huang and M.S. El-Genk, Heat Transfer of an Impinging Jet on a Surface, *Int. J. Heat and Mass transfer,* vol. 37, no. 13, pp. 1915-1923, 1994.

[12] T.M. Liou, W.B. Wang and Y.J. Chang, Holographic Interferometry Study of Spatially Periodic Heat Transfer in a Channel with Ribs Detached from One Wall, *Int. J. Heat and mass Transfer,* vol. 117, pp. 32–39, 1995.

[13] T.M. Liou, W.J. Shuy and Y.H. Tsao, Effect of Rib Height and Pitch on the Thermal Performance of a Passage Disturbed by Detached Solid Ribs, *Int. J. Turbomach*, Vol. 12, pp. 581–588, 1998.

[14] J.P. Tsia and J.J. Hwang, Measurements of Heat Transfer and Fluid Flow in a Rectangular Duct with Alternate Attached–Detached Rib Array, *Int. J. Heat Mass Transfer,* vol. 42, pp. 2071–2083, 1999.

[15] V.V. Katti and S.V. Prabhu, Heat Transfer Enhancement on a Flat Surface with Axisymmetric Detached Ribs by Normal Impingement of Circular Air Jet, *Int. J. Heat and Fluid Flow*, vol. 29, pp. 1279-1294, 2008.

[16] Y. Shi, M.B. Ray and A.S Mujumdar, Computational Study of Impingement Heat Transfers Under a Turbulent Slot Jet, *Ind. Eng. Chem*., vol. 41, pp. 4643-4651, 2002.

[17] M. Pathak, A. Dewan and A.K. Dass, Computational Prediction of a Slightly Heated Turbulent Rectangular Jet Discharged into a Narrow Channel Cross Flow Using Two Different Turbulence Models*, Int. J. Heat Mass Transfer*, vol. 49, pp. 3914-3928, 2006.

[18] C. Sak, R. Liu, D.S.-K. Ting and G.W. Rankin, Role of Turbulent Length Scale and Turbulent Intensity on Forced Convection from a Heated Horizontal Circular Cylinder, *Experimental Thermal and Fluid Sciences*, vol. 31, pp. 279-289, 2007.

[19] A. Dewan, Tackling Turbulent Flows in Engineering, *Springer*, Germany, 2011.

[20] B.E. Launder and D.B. Spalding, Lectures in Mathematical Models of Turbulence; *Academic Press, London, England*, 1972.

[21] T-H. Shih, J. Zhuand and J.L. Lumley, A New Reynolds Stress Algebraic Equation Model, *Computer Methods in Applied Mechanics and Engineering*, vol. 125, pp. 287-302, 1995.

[22] V. Yakhot, S. A. Orszag, S. Thangam, T. B. Gatski, and C. G. Speziale, Development of Turbulence Models for Shear Flows by a Double Expansion Technique, *Physics of Fluids* A, vol. 4, no. 7, pp. 1510-1520, 1992.

[23] D.C Wilcox, Turbulence Modeling for CFD, DCW Industries*, Inc., La Canada, California, USA*. 1998.

[24] S.V. Patankar, Numerical Heat Transfer and Fluid Flow, *Taylor & Francis, USA*, 1980.

Authors' information

Department of Applied Mechanics, Indian Institute of Technology Delhi, New Delhi – 110016, India.



Anupam Dewan is a Professor, Department of Applied Mechanics, Indian Institute of Technology Delhi. He obtained his Bachelor's degree in Mechanical Engineering from Kurukshetra University, India and Master's and Ph.D. in Mechanical Engineering from Indian Institute of Science Bangalore. He was a Professor of Mechanical Engineering at Indian Institute of Technology Guwahati before joining IIT Delhi in May 2009. His areas of specialization include Computational Fluid Dynamics and Heat Transfer, Mathematical Modelling of Engineering Turbulent Flows, Turbulent Convective Heat Transfer and Heat Transfer Enhancement. He has co-authored more than eighty refereed journal and conference publications, which include three review articles in leading international journals on different aspects of computational fluid mechanics and heat transfer. He has recently authored a book "Tackling Turbulent Flows in Engineering" published by Springer.



Deep Prakash Gupt has completed has Master of Technology degree from Department of Applied Mechanics, Indian Institute of Technology Delhi. His M.Tech. project was entitled "Computational Study of Enhancement of Heat Transfer Through Air Jet impingement by Using axisymmetric Detached Ribs". He obtained his Bachelor of Technology in Manufacturing Technology from U.P. Technical University, Lucknow, India.



Sanjeev Sanghi obtained his Bachelor's degree in Mechanical Engineering from the Indian Institute of Technology Kanpur. He continued his education further at Cornell University and The Levich Institute of City University of New York from where he obtained his MS and PhD respectively. He is Professor in the Applied Mechanics Department at the Indian Institute of Technology Delhi. His areas of interest include Numerical and Analytical Studies of Turbulent Flows, Chaos and Dynamical Systems, Finite Element Method (FEM), Educational Software, Proper Orthogonal Decomposition. He has published papers in leading journals like Journal of Fluid Mechanics, Journal of Computational Physics, Physics of Fluids, Chaos, AIAA Journal, ASME Journal of Heat Transfer, Journal of Sound and Vibration, Computers and Structures and Computers and Fluids.

PREPRINT

Copyright © 2013 Praise Worthy Prize S.r.l. - All rights reserved

International Review of Mechanical Engineering
(IREME)

(continued from outside front cover)

Solar Assisted Air-Conditioner, Simulation and Economic Analysis at Four-Seasonal Climate 350
by P. Ooshaksaraei, K. Sopian, R. Zulkifli

Performance of Single Pass Photovoltaic Thermal Solar Collector with Bifacial Solar Cells 358
by P. Ooshaksaraei, K. Sopian, R. Zulkifli, Saleem H. Zaidi, R. Sirwan

Swirl Analysis in Round Tubes with Partially Short Length Twisted Tapes with Turbulent Flow 364
by R. J. Yadav, A. S. Padalkar

Investigation on Thermal Balance of CI Engine Fuelled by Pongamia Pinnata Biodiesel and Hydrogen as Secondary Fuel 375
by C. Jegadheesan, P. Somasundaram

Optimization of Rectangular Microchannel Depth Under Forced Convection Heat Transfer Condition 379
by B. S. Gawali, D. A. Kamble

Effects of the Heated Surface on the Unsteady Two Dimensional Natural Convection in Enclosures Bounded by Two Paraboloids of Revolution 384
by Samba Dia, Cheikh Mbow

REPRINT

Abstracting and Indexing Information:

Cambridge Scientific Abstracts (CSA/CIG)
Academic Search Complete (EBSCO Information Services)
Elsevier Bibliographic Database SCOPUS
Index Copernicus (Journal Master List): ***Impact Factor 6.46***

Autorizzazione del Tribunale di Napoli n. 6 del 17/01/2007

REPRINT



1970-8734(201302)7:2;1-Q

Copyright © 2013 Praise Worthy Prize S.r.l. - All rights reserved